Proceedings World Geothermal Congress 2020+1
Reykjavik, Iceland, April - October 2021

Fracture Wall Crystallography Control on Mineral Scaling in Geothermal Reservoirs: Preliminary Results

Aisling Scully[1], David D. McNamara[2], Sandra Piazolo[3] and Isabelle Chambefort[4]

[1]School of Biological, Earth and Environmental Sciences, University College Cork, Ireland

[2]University of Liverpool, United Kingdom

[3]University of Leeds, United Kingdom

[4]GNS Science, New Zealand

aislingscully.333@gmail.com

Keywords: calcite, fracture sealing, nucleation, microstructure, crystallography, geothermal, reservoir, scaling, EBSD

ABSTRACT

Efficient and sustainable production of geothermal resources are dependent on several factors, most critically, the maintenance of open structural pathways for fluid flow. An interconnected fracture system is essential for heat and fluid migration within a reservoir, particularly in crystalline host rocks where intrinsic permeability is low. Over time, numerous fluid-rock interactions within these reservoirs lead to mineral nucleation and growth, eventually resulting in partial or complete fracture sealing i.e. reservoir scaling. This work presents initial findings of microstructural characterisation of calcite scaling in a geothermal system in Kibiro, Uganda. Electron Backscatter Diffraction (EBSD) reveals that calcite can display a special orientation relationship with quartz involving the calcite m and quartz a directions. However, when adularia is present at the fracture wall interface alongside quartz, calcite will nucleate preferentially on adularia via a special orientation relationship involving the c and a directions of both minerals. This indicates that adularia requires less energy for nucleation and attachment of calcite molecules than quartz. Preliminary observations suggest that it is not simply host rock lithology determining nucleation and subsequent growth of these fracture sealing minerals, but the crystal lattice arrangement of specific minerals in the fracture wall assemblage exerting a preferential control.

1. INTRODUCTION

1.1 Background

Calcite precipitation, a common form of mineral scaling in fractured geothermal reservoirs, is the process by which calcite crystals nucleate and grow out of circulating fluids within fluid flow pathways (Taron and Elsworth, 2009). Fracture scaling occurs via mineral nucleation by particle attachment, whereby a small precursor mineral or mineral seed bonds onto other particles, either present in the fracture wall surface, or onto particles within the fluid (Li et al., 2012; Gebauer et al., 2014; Hamm et al., 2014; De Yoreo et al., 2015). Subsequently, nucleated minerals will grow into the open fracture, eventually leading to full closure. Mineral scaling presents a problem in the geothermal energy industry, as over time, scaling in a fractured reservoir will inhibit fluid flow and reduce production and resource efficiency (Batzle and Simmons, 1976, Dobson et al., 2003; Genter et al., 2010; McNamara et al., 2016; Griffiths et al., 2016). Despite the importance of reservoir scaling, the physical mechanisms which govern mineral nucleation and growth scaling processes in natural geological systems are still poorly characterised. Furthermore, the physio-chemical conditions that control these physical nucleation and growth processes are not yet understood.

Fracture sealing mechanisms have been a pressing research topic since the early 1970's (Batzle and Simmons,1976). Both fluid-rock interactions and the wide array of physical and chemical conditions which occur in geothermal systems can affect the style of nucleation and mineral growth in a fracture. While chemical supersaturation of the fluid or changes in fluid temperature and pressure are among the most common factors suggested to influence mineral scaling (Fisher and Brantley, 1992; Sonney and Mountain, 2013), other contributors are known to exert some level of control also, including fluid velocity (Okamoto and Tsuchiya, 2009), fracture wall petrography/chemistry (Landrot et al., 2012), microbial influences (Mountassir et al., 2014), fracture wall topography (Tartakovsky et al., 2007; Huber et al., 2014: Liu et al., 2015), changes in Ph/Eh (Kaczmarek and Thornton, 2017) and the physical attributes of the mineralising crystal (Urai et al., 1991). With modern advances in microscopy, such as electron backscatter diffraction and energy dispersive x-ray spectroscopy, mineral crystallography and chemistry characterisation is more readily available, opening up new research pathways to explore fracture sealing processes (Prior et al., 2009; Bons et al., 2012). The application of such techniques to understanding mineral scaling in fractured geothermal systems is in its infancy, but the few studies that exist show its potential (McNamara et al. 2016; Griffith et al., 2016).

Many chemical and physical solutions have been applied to remedy the scaling issue in geothermal systems, including, chemical scale inhibitors and stimulation (Evanoff et al., 1995; Mella et al., 2006; Portier et al., 2009), magnetic treatments (Parsons et al., 1997), and pressure control methods (Corsi, 1986; Antony et al., 2011), while controls on the scaling mineral nucleation and growth process itself have been explored via both experimental research (Rothbaum et al., 1979; Gallup et al., 2003; Izgec et al., 2005) and numerical modelling (Arnórsson, 1989; García et al., 2006; Kiryukhin et al., 2004). This microanalytical study seeks to determine crystallographic controls on calcite nucleation and growth in geothermal fractures, and further our understanding of what factors promote or inhibit these processes. By determining the physical controls on geothermal reservoir calcite scaling, and the conditions at which they occur, we aim to assist with the development of future tools for preventing, inhibiting, or remediating this problem.

1.2 Geological Setting

The Albertine Rift System (ARS), situated at the boundary between the Democratic Republic of Congo and Uganda (Figure 1), is the northernmost segment of the ~2100km set of rifted basins which make up the western limb in the East African Rift System (EARS). This intracontinental basin sequence is crosscut by multiple transfer zones (Morley, 1999) and contains two distinct rift zones which are propagating towards each other, adjacent to Lake Albert and Lake Edward respectively (Morley 1999, Koehn et al., 2010). The study area at Kibiro is located along the Toro-Bunyoro fault (Figure 1B), which is contained within the northern half of the ARS, striking approx. NE-SW and bordering the eastern edge of Lake Albert. The main Toro-Bunyoro fault cuts directly through exposed Precambrian basement blocks, comprised of multiple crystalline units ranging in composition from acidic granulties in the north, to TTG granatoids in the south (Virransalo et al., 2012).

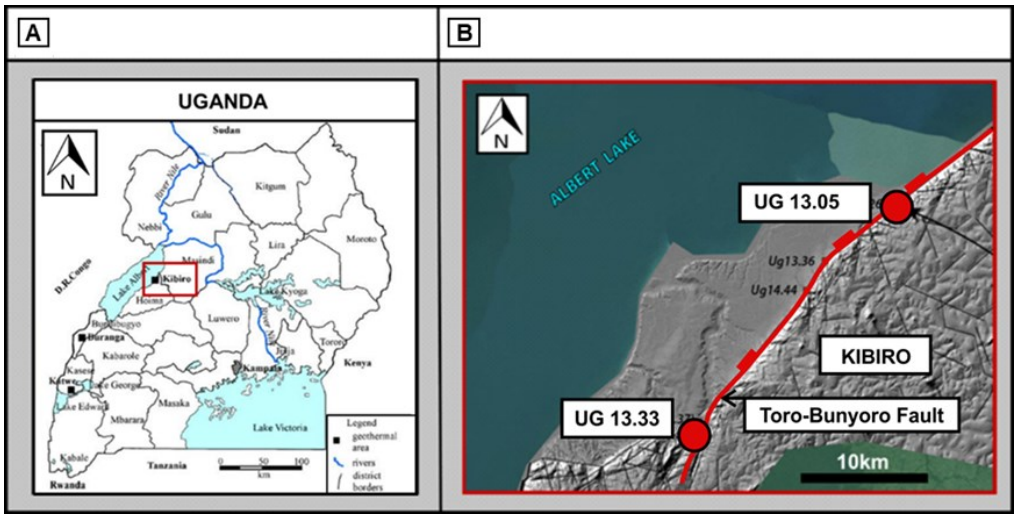

Figure 1: A) From Bahati (2012). The figure above depicts the boundaries of Uganda, with the Kibiro geothermal area highlighted within the red box. This is the location of the study area. B) Modified from Walters (2015). This inset shows the individual sample sites along the Toro-Bunyoro fault, which runs adjacent to Lake Albert in the West.

Although there is no evidence of magmatism near the Lake Albert rift zone, geothermal activity is observed at the Kibiro site which contains a significant geothermal gradient (Bahati, 2012). Multiple zones of paleo and present-day circulation, evidenced by the presence of hydrothermal vents and fluid seeps on faults, and hydrothermal alteration of the country rock, have been noted in the Toro – Bunyoro area (Walters, 2016). Hydrothermal fluids circulate within the subsurface via heavily fractured basement rocks controlled strongly by regional structures (Walters, 2016). Electrical resistivity surveying (Bahati, 2012), supported by 300m drill holes, show fluids can circulate to large depths by these structures. Integrated fluid inclusion analysis, isotope studies, microstructural observations, geochemical analysis, and petrological investigation carried out by Walters (2016) identifies four main stages of fluid circulation. The first phase (Figure 2A), is characterised by the deposition of chlorites and sulphides, as well as a slightly later generation of high temperature calcite (170-200°C). The following phases consist of a high temperature mineralisation of adularia, followed by polyphase mineralisation of lower temperature (<100°C) calcite.

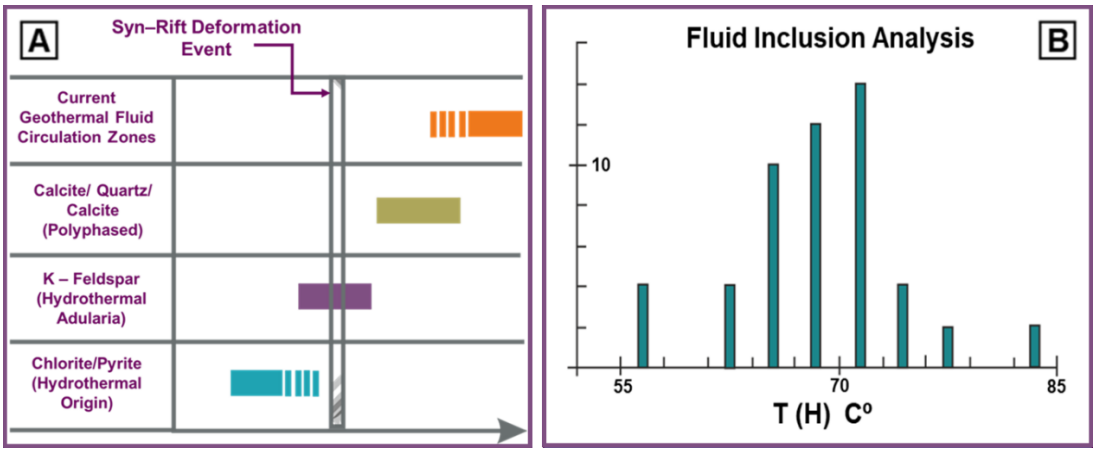

Figure 2. Modelled after (Walters, 2016). A) Diagram showing the four stages of fluid circulation in the Kibiro geothermal zone. B): Fluid inclusion results from late stage calcite mineralisation placing formation temperatures at approx. 70°C.

2. MATERIALS AND METHODS

2.1 Samples and Sample Preparation

The vein samples taken at site UG 13.05 and UG 13.33 were sampled approx. 20km apart and were situated adjacent to the main fault core (Figure 1B), where both vein sets were hosted in an Archean quartzo-feldspathic gneiss unit (Walters, 2016). Thin sections analysed in this work measured 30 μm in thickness and underwent diamond polishing (1 μm). This was followed by mechanical and chemical polishing using colloidal silica, to promote sharper pattern collection for mineral indexing during EBSD (Prior et al.1996). Each of the thin sections was coated in approx. 10 nm of carbon, and copper tape was applied to the edges of each slide. Both copper tape and carbon coating were used to reduce build-up of electron charge on the sample surface during EBSD acquisition.

2.2 Electron Backscatter Diffraction (EBSD)

EBSD data collection was done using a FEI Quanta 650: Field Emission Scanning Electron Microscope at the University of Leeds, United Kingdom. During acquisition, a working distance of ~20mm was used, with an acceleration voltage of 25kV and a beam current of ~50 nA. EBSD map data was collected using AZTec. All initial processing was carried out using AZTec, while post acquisition processing was done using HKL Channel5. Data was collected at a step size of 10 μm.

EBSD phase ID and orientation relationship component maps were created using the Tango software module from HKL Channel 5, and the interphase relationships between the fracture wall and vein fill minerals were analysed. Orientation relationships were examined for all crystallographic plane/direction pairings between fracture wall quartz/vein calcite and vein adularia/vein calcite. The misorientation distribution for crystallographic directions between different phases is examined to identify any special orientation relationships.

3. RESULTS

3.1 Vein 13.33 – Relay Zone

3.1.1 Petrography

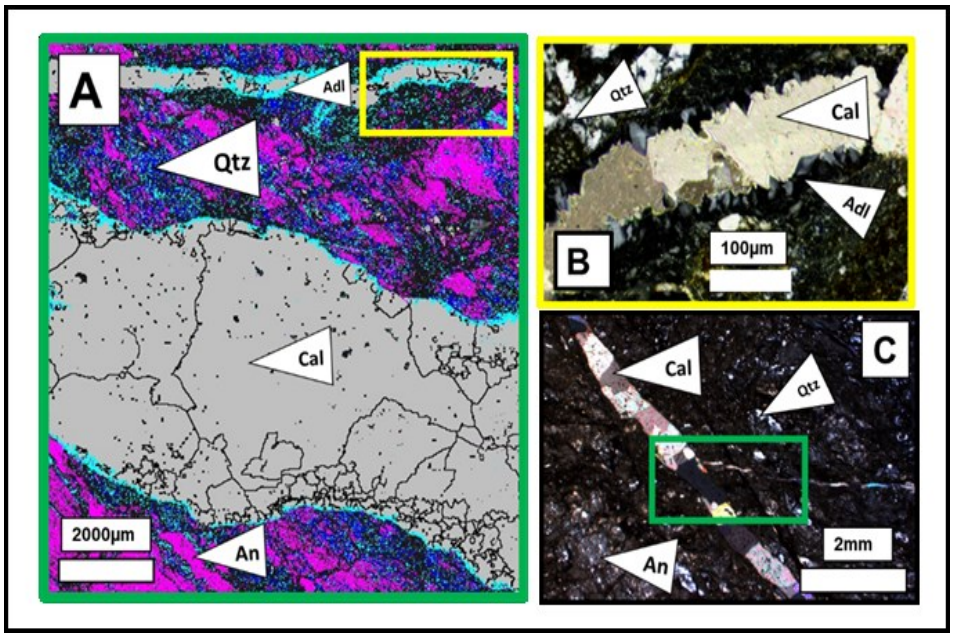

Figure 3: A) Phase ID EBSD map of sample UG 13.33 displaying a first-generation calcite vein hosted in deformed quartzo feldspathic gneiss (blue and pink) and the smaller second-generation calcite vein. Calcite is in grey, quartz is in blue, anorthite is in pink and adularia shown in turquoise. B) Close up image of the secondary vein wall/mineral interface showing adularia phase adjacent to fracture and calcite mineralisation within. C) Light microscope image in XPL showing dark groundmass cross cut by multiple generations of calcite veining.

Sample 13.33 is made up of a foliated quartzo-feldspathic gneiss made up of predominately quartz and anorthite clasts, with some small microcline clasts present (Figure 3A). Anorthite clasts are small (sub mm to 0.2 mm) and show evidence of alteration and replacement to chlorite. Quartz clasts are larger (sub mm – 2 mm) and are highly deformed. There are multiple stages of veining in this sample, an older vein, Vein I, <2mm in width, filled with highly twinned calcite that displays sericitic alteration (Figure 3), and a younger stage vein, Vein II, that displays multiple scaling events the first of which is adularia, followed by a later scaling of undeformed calcite (Figure 3B).

3.1.2 EBSD

In Vein I, scaling calcite displays a special orientation relationship with quartz in the fracture wall rock. This relationship is defined by a 45 misorientation of the calcite <m> direction on the quartz <a> direction (Figure 4). In Vein II, this special orientation relationship between scaling calcite and wall rock quartz is absent (Figure 5). When the calcite/adularia phase relationship is examined in Vein II, a strong special orientation relationship is observed between these minerals defined by a misorientation of 35 of the calcite

<a> direction on the adularia <a> direction. Figure 6 shows that the majority of calcite/adularia interfaces display this special orientation relationship.

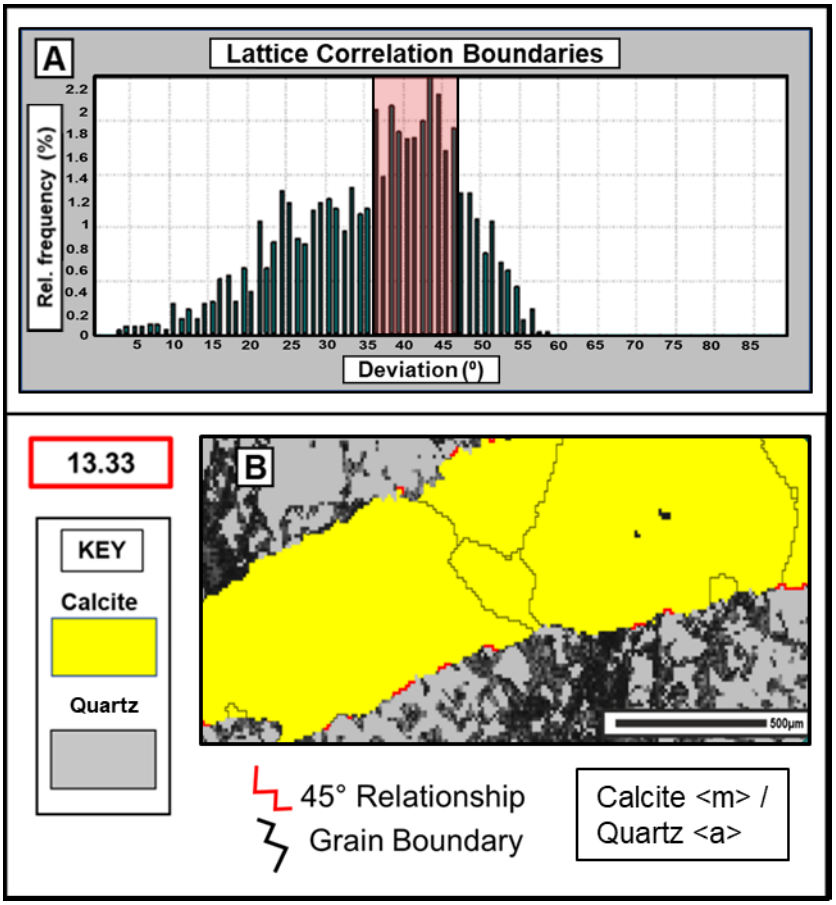

Figure 4: The figure above quantifies the geometric relationship between Calcite <m> and Quartz <a> crystallographic directions. A) Graph displaying the relative frequency of the angle of misorientation/deviation in Vein I between two mineral phases in the <a> and <m> directions, Quartz and Calcite. B) EBSD phase map showing host rock quartz in grey and vein calcite in yellow, with the special orientation relationship of 45° misorientation highlighted in red.

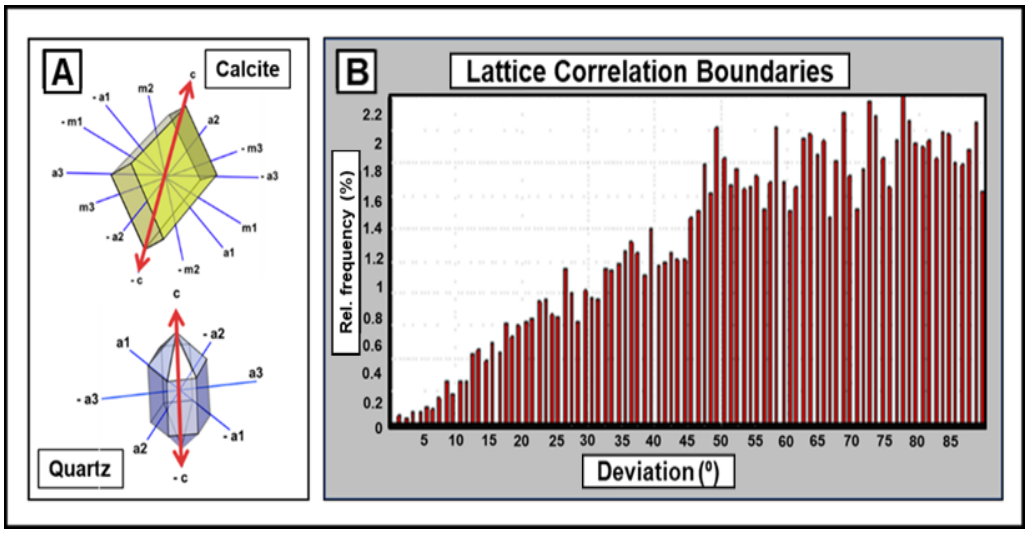

Figure 5: The figure above quantifies the geometric relationship between Calcite <c> and Quartz <c> crystallographic directions. A) Crystallographic blueprint of Calcite (Trigonal) and Quartz (Trigonal) with relevant directions highlighted. B) Graph displaying the relative frequency of the angle of deviation in Vein II between two mineral phases in the <c> direction, Quartz and Calcite.

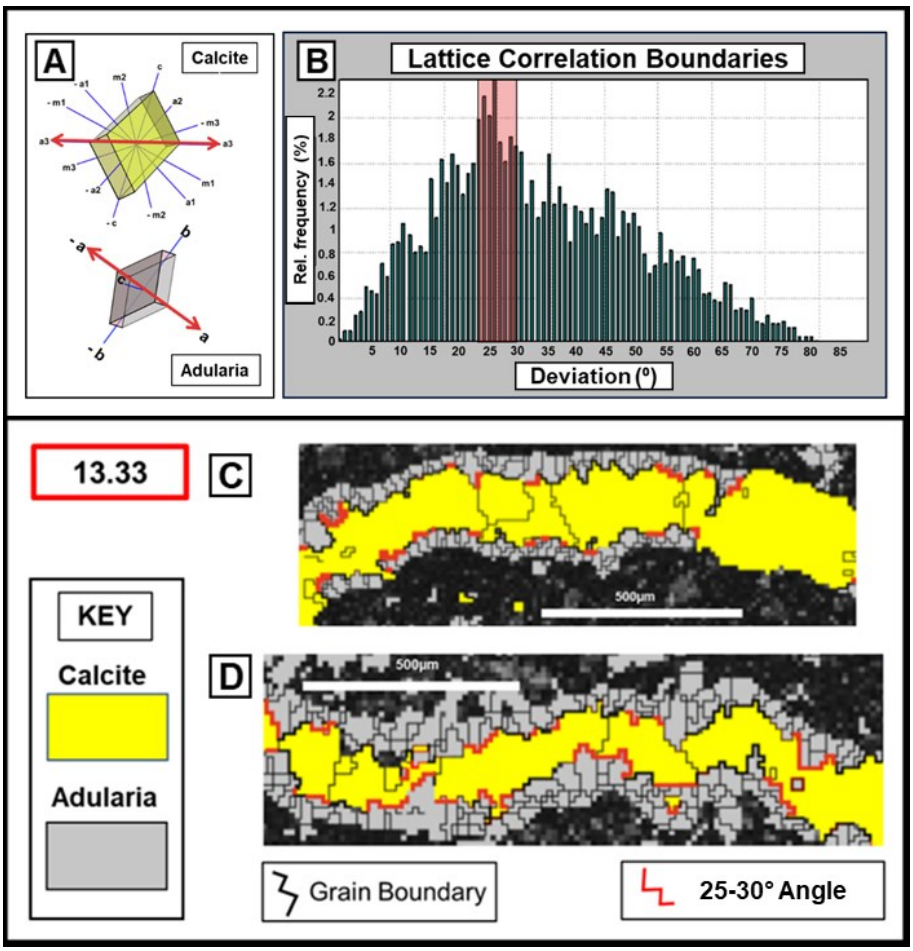

Figure 6: The figure above quantifies the special orientation relationship between Calcite <a> and Adularia <a> crystallographic directions in Vein II. A) Crystallographic blueprint of Calcite (Trigonal) and Adularia (Monoclinic) with relevant directions highlighted. B) Graph displaying the relative frequency of the angle of deviation in Vein II between two mineral phases in the <a> direction, Adularia and Calcite. C/D) EBSD phase maps of Vein II, highlighting the special orientation relationship between Calcite <a> and Adularia <a> with a misorientation of 25-30°. Mineral phases are calcite (yellow) and adularia (grey) with the orientation relationship boundaries between phases shown in red.

3.2 Vein 13.05 – Fault Core

3.2.1 Petrography

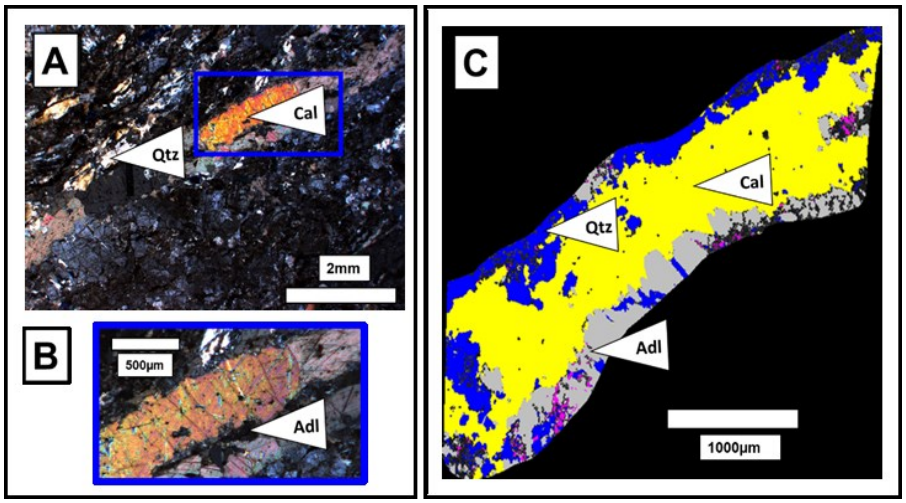

Figure 7: A) Light microscope image of Sample 13.05 in XPL showing the main calcite vein hosted in deformed quartzo feldspathic gneiss. B) Close up image of the vein wall/mineral interface showing adularia phase adjacent to fracture. C) Phase ID EBSD map of same calcite vein seen in A and B, showing quartz in blue, adularia in grey and calcite in yellow.

Sample 13.05 is predominantly comprised of a fine-grained, dark matrix with cataclastic fault gouge texture throughout, within quartzo-feldspathic gneiss, which is interspersed with calcite veins (Figure 7A). Clasts can be observed in the fault gouge and are primarily composed of quartz and feldspars, typically <2 mm in size which show evidence of brittle damage. The calcite veins within this sample (Figure 7A) range in width between 0.2 mm and 1mm, with some of the smaller veins also containing the hydrothermal k-feldspar, adularia. Adularia is also found as a hydrothermal alteration mineral within the wall rock surrounding some of the hydrothermal veins.

3.2.2 EBSD

Lattice correlation boundary maps and misorientation distribution analyses reveal a special orientation relationship between adularia and calcite (Figures 8 and 9). This is defined by both a misorientation of 85 of the calcite <c> direction on the adularia <c> direction, and a 25-30 or a ~65 misorientation of the calcite <a> direction on the adularia <a> direction. A further special orientation relationship is also observed between vein calcite and quartz in the fracture wall, defined by a 45 misorientation of the calcite <c> direction on the quartz <c> direction (Figure 10). This relationship is minor and occurs less frequently in this sample compared to the interface relationship between calcite and adularia.

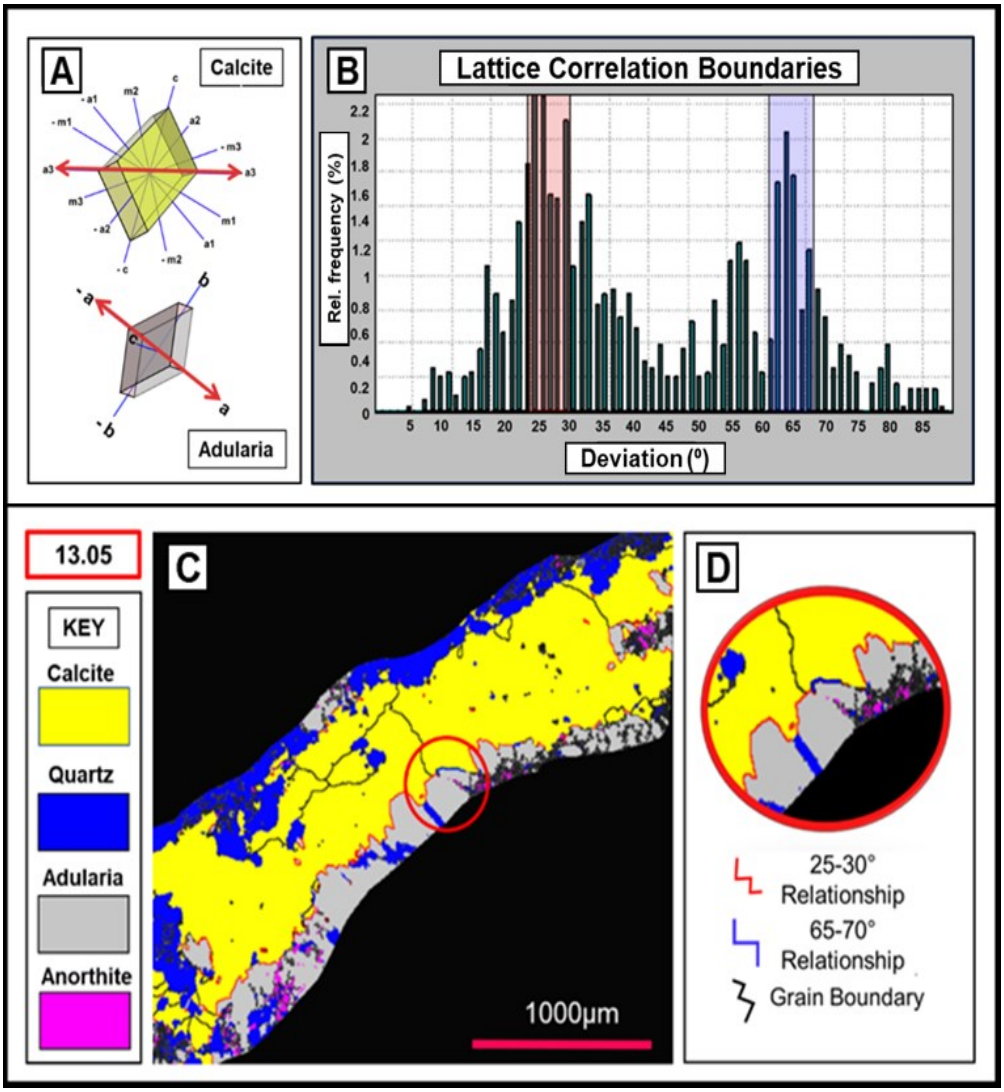

Figure 8: The figure above quantifies the special orientation relationship between vein calcite <a> and alteration mineral adularia <a> crystallographic directions. A) Crystallographic blueprint of calcite (trigonal) and adularia (monoclinic) with relevant directions highlighted. B) Graph displaying the relative frequency of the angles of deviation/misorientation of 25-30° and the lesser relationship of 65-70° between calcite and adularia <a> directions. C) EBSD phase map displaying the special orientation relationship between calcite <a> on adularia <a> by misorientations of both 25-30° and 65-70°, mineral phases are calcite in yellow, quartz in blue, adularia in grey and anorthite in pink. D) Cut-out of the special relationships in more detail.

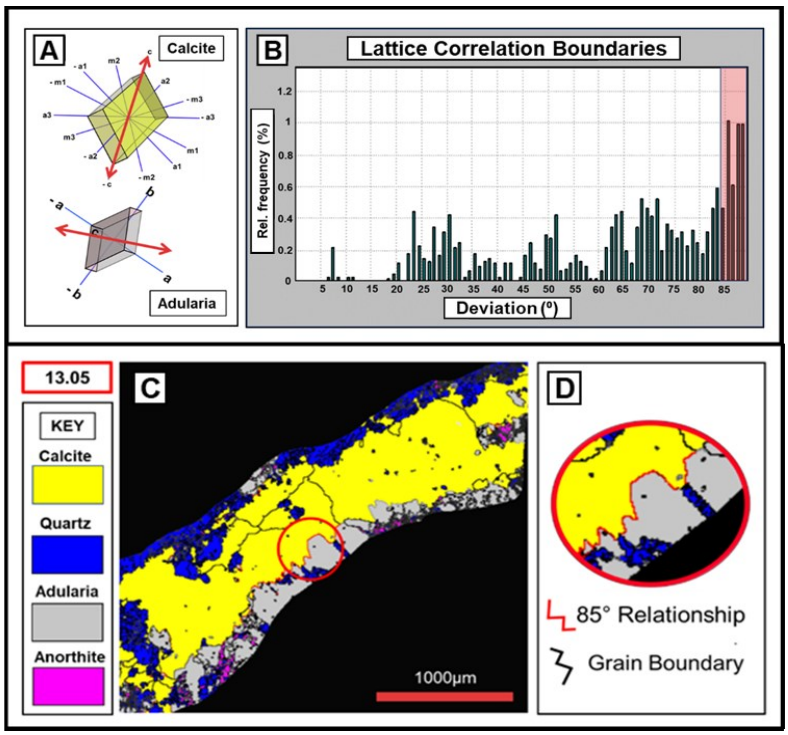

Figure 9: The figure above quantifies the special orientation relationship between vein calcite <a> and alteration mineral adularia <a> crystallographic directions. A) Crystallographic blueprint of calcite (trigonal) and adularia (monoclinic) with relevant directions highlighted. B) Graph displaying the relative frequency of the angle of deviation/misorientation of 85° between calcite and adularia <a> directions. C) EBSD phase map displaying the special orientation relationship between calcite <a> on adularia <a> by misorientation of 85°, mineral phases are calcite in yellow, quartz in blue, adularia in grey and anorthite in pink. D) Cut-out of the special relationships in more detail.

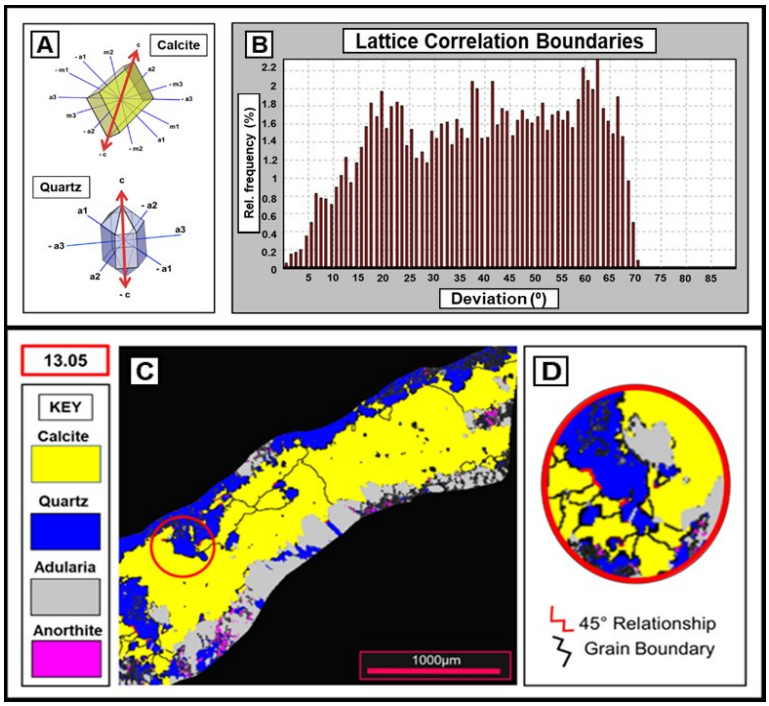

Figure 10: The figure above quantifies the special orientation relationship between calcite <c> and quartz <c> crystallographic directions. A) Crystallographic blueprint of calcite (trigonal) and quartz (trigonal) with relevant directions highlighted. B) Graph displaying the relative frequency of the angle of deviation/misorientation of 45° between quartz and calcite in the <c> direction. C) EBSD phase map displaying the special orientation relationship between calcite <c> on quartz <c> by a misorientation of 45°, mineral phases are calcite in yellow, quartz in blue, adularia in grey and anorthite in pink. D) Cut-out of the special relationship in more detail.

4. DISCUSSION

Our data shows that there is a clear crystallographic control on the nucleation and subsequent growth of calcite in geothermal veins in the Kibiro area. From previous work (Walter, 2016) we know vein calcite precipitation occurred in two stages in this region, an older, high temperature stage (170-200°C) and a younger, lower temperature stage (~70°C). Out of the two sites examined, only one location (UG 13.33) shows evidence of the older stage, high temperature vein calcite precipitation. In this vein our EBSD data shows that scaling calcite shows a preference to nucleate on quartz in the fracture wall via a special orientation relationship (defined by a 45° misorientation of calcite <m> direction on the quartz <a direction>). This shows a clear control on calcite scale nucleation by the mineralogy of the fracture wall rock.

These older calcite sealed fractures are cross-cut by a younger generation of fractures, which are present in both samples. The younger fractures in sample UG 13.33 are subsequently sealed first by adularia, followed by a later calcite event (low temperature stage, ~70°C). Calcite precipitation in these younger fractures occurs on both quartz and adularia. Adularia is also present as a wall rock alteration mineral in sample UG 13.05. EBSD data shows a special orientation relationship between vein calcite and both forms of adularia. There is a common special orientation relationship between calcite and both alteration and vein adularia, which is the 25-30° misorientation of the calcite <a> direction on the adularia <a> direction. This relationship is ubiquitous across all samples. A second, less common special orientation relationship exists between alteration adularia and vein calcite, defined as a misorientation of ~65° of the calcite <a> direction on the adularia <a>. Additionally, in this same sample there is a further, subordinate special orientation relationship between alteration adularia and vein calcite, defined by the <c> directions of calcite and adularia with an 85° misorientation. Adularia appears to be exerting control over calcite nucleation at all localities, with slightly different geometric controls depending on its occurrence, vein or host-rock alteration. This could be a result of textural and morphological differences between the two forms of adularia, or available free-space for calcite growing from these different adularia forms. Future work will explore this theory in greater detail.

A minor special orientation relationship is observed in one example (UG 13.05) between quartz and calcite, where the calcite <c> direction is misoriented at an angle of 45° to the quartz <c> direction. So while calcite nucleation is occurring on both adularia and quartz sites, by far the adularia surfaces seem to be preferred, particularly for calcite <a> via a 25°- 30° misorientation on the adularia <a> direction. These findings further demonstrate control on calcite nucleation in geothermal fractures by the mineralogy and of the wall rock.

Observations from both veins infer that calcite prefers to nucleate on adularia over quartz, when both are available in the fracture wall. However, we do observe that calcite will nucleate on quartz when adularia is absent. Calcite is known to prefer heterogeneous particles rather than homogenous for attachment i.e. non-calcite (Gránásy et al., 2007; De Yoreo et al., 2015), so both quartz and adularia should potentially be viable sites for attachment. However, the findings of our study show a clear preference for nucleation on adularia at both localities, therefore we must consider other factors contributing to the selection process of calcite as it chooses adularia over quartz. As mentioned previously, fluid inclusion work carried out by Walter (2015) places the later stage calcite formation temperatures between 55 and 70 °C, a low temperature range for geothermal calcite precipitation. Low temperature regimes affect mineral nucleation and crystallisation rates by reducing factors such as kinetic energy, diffusion rate, and supersaturation, therefore activation occurs less readily than in a higher temperature environment (Dalas and Koutsoukos, 1990; Schobesberger et al., 2010; Mc Graw et al., 2017). In this type of low temperature regime, where nucleation activation energy must work harder to overcome the free energy within the system, factors such as interfacial surface tension and surface area of the potential nucleation site become more important factors in the path to successful nucleation (Li et al., 2012; Gebauer et al., 2014; Hamm et al., 2014; De Yoreo et al., 2015). In addition to this, recent work on nucleation theory proposes that pre-nucleation, the mineral seed or precursor will rotate within the fluid until a favourable lattice alignment is found for attachment (Li et al., 2012), so good structural compatibility between the mineral seed nuclei and the attachment site can play a significant role (Jun et al., 2016).

If we apply the idea of limiting factors such as varying surface energies or the necessity for favourable physical alignment for nucleation to our own results, a common element emerges. If calcite is indeed attempting to attach to a surface with preferable conditions for nucleation, it is possible that the main significant difference between quartz and adularia is crystal structure of the minerals themselves. Higher crystallographic complexity has a greater potential to contain multiple crystal faces, smaller surface areas on these faces, and differing growth directions associated with variable growth rates in comparison to simpler crystallographic forms. This can result in unfavourable surface tensions discouraging nucleation (Che et al., 1998; Michaelides and Scheffler, 2012; Ringe et al, 2013). Adularia, being monoclinic by nature and more simplistic structurally, naturally provides fewer possible geometric choices in terms of available attachment surfaces, and as such more favourable surface energies, thus promoting itself as a nucleation site. This hypothesis is supported by similar behaviour in previous experimental studies, where it is observed that calcite preferentially nucleates on mica, another crystallographically simplistic mineral, over quartz, thereby highlighting the importance of interfacial energies in the nucleation process (Li et al., 2014). In addition to this, with its limited choice of orientations to use as a template, adularia most likely has a higher probability for favourable alignment while the particle rotates and matches up pre-nucleation (Li et al. 2012), than the more structurally complex trigonal crystal, quartz.

Attachment onto selective crystal faces has been observed previously by Zhang et al. (2017) and was labelled as oriented attachment, where the adhesion free energy on the attachment surface increases dramatically when lattice alignment occurs. Our results show a strong alignment of the <a> directions in both localities for calcite and adularia, a repeated behaviour which is not observed in the quartz/calcite relationship. The <a> lattice direction appears to be the dominant special orientation direction, so it is potentially the geometric combination with the lowest formation energy atomically (Zhang et al., 2017). When we compare the two different calcite phases, high temperature (170-200°C) nucleation on quartz and lower temperature (approx. 70°C) nucleation on adularia, it could be argued that the higher kinetics in the hotter system significantly affect the criteria for nucleation. Crystallography does not appear to be as dominant a factor in the older calcite mineralisation as it does in the lower temperature event, where the smallest difference in atomic energies can direct mineral attachment onto specific surfaces. However, in systems where this atomic energy is critical for successful calcite nucleation, it seems highly probable that crystallography plays an important role in this geothermal scaling process.

CONCLUSIONS

Identifying adularia as a control for mineral scaling and understanding the role that temperature and crystallography play in this process is crucial information for furthering our understanding of reservoir scaling processes. Due to the undesirable presence of calcium carbonate scale in many geothermal fields worldwide, the identification of a controlling factor such as this may be key to developing future reservoir scaling solution toolkits. Temperature of reinjected fluids is a parameter which can be regulated, as is identifying reservoir lithologies and potentially searching for the presence of adularia in a system. While these factors are only two in a range of controls, identifying them is another step along the road to more efficient, practical management of geothermal production issues.

REFERENCES

Antony, A., Low, J. H., Gray, S., Childress, A. E., Le-Clech, P., and Leslie, G.: Scale formation and control in high pressure membrane water treatment systems: a review. Journal of membrane science, 383(1-2), (2011), 1-16.

Arnórsson, S.: Deposition of calcium carbonate minerals from geothermal waters—theoretical considerations. Geothermics, 18(1-2), (1989), 33-39.

Batzle, M.L. and Simmons, G.: Microfractures in rocks from two geothermal areas. Earth and Planetary Science Letters, 30(1), (1976), pp.71-93.

Bons, P.D., Elburg, M.A. and Gomez-Rivas, E.: A review of the formation of tectonic veins and their microstructures. Journal of Structural Geology, 43, (2012), pp.33-62.

Che, J. G., Chan, C. T., Jian, W. E., and Leung, T. C.: Surface atomic structures, surface energies, and equilibrium crystal shape of molybdenum. Physical Review B, 57(3), (1998), 1875.

Corsi, R.: Scaling and corrosion in geothermal equipment: problems and preventive measures. Geothermics, 15(5-6), (1986), 839-856.

Dalas, E., and Koutsoukos, P. G.: Calcium carbonate scale formation and prevention in a flow-through system at various temperatures. Desalination, 78(3), (1990), 403-416.

Dobson, P.F., Kneafsey, T.J., Hulen, J. and Simmons, A.: Porosity, permeability, and fluid flow in the Yellowstone geothermal system, Wyoming. Journal of Volcanology and Geothermal Research, 123(3-4), (2003), pp.313-324.

De Yoreo, J. J.; Waychunas, G. A.; Jun, Y.-S.; and Fernandez-Martinez, A.: In situ Investigations of Carbonate Nucleation on Mineral and Organic Surfaces. Rev. Mineral. Geochem., 77, (2013), 229−257.

Evanoff, J., Yeager, V., and Spielman, P.: Stimulation and damage removal of calcium carbonate scaling in geothermal wells: a case study. In: Proceedings of the 1995 World Geothermal Congress, Florence, Italy, (1995), pp. 2481–2485.

Fisher, D. M., and Brantley, S. L.: Models of quartz overgrowth and vein formation: deformation and episodic fluid flow in an ancient subduction zone. Journal of Geophysical Research: Solid Earth, 97(B13), (1992), 20043-20061.

Gallup, D. L., Sugiaman, F., Capuno, V., and Manceau, A.: Laboratory investigation of silica removal from geothermal brines to control silica scaling and produce usable silicates. Applied Geochemistry, 18(10), (2003), 1597-1612.

García, A. V., Thomsen, K., and Stenby, E. H.: Prediction of mineral scale formation in geothermal and oilfield operations using the Extended UNIQUAC model: Part II. Carbonate-scaling minerals. Geothermics, 35(3), (2006), 239-284.

Gebauer, D. and Cölfen, H.: Prenucleation clusters and non-classical nucleation. Nano Today, 6(6), (2011), pp.564-584.

Genter, A., Evans, K., Cuenot, N., Fritsch, D., and Sanjuan, B.: Contribution of the explora- tion of deep crystalline fractured reservoir of Soultz to the knowledge of enhanced geothermal systems (EGS). Compt. Rendus Geosci. 342, (2010), 502–516.

Gránásy, L., Pusztai, T., Saylor, D., and Warren, J. A.: Phase field theory of heterogeneous crystal nucleation. Physical review letters, 98(3), 035703, (2006).

Griffiths, L, M. J. Heap, F. Wang, D. Daval, H. A. Gilg, P. Baud, J. Schmittbuhl, and A. Genter.: Geothermal implications for fracture-filling hydrothermal precipitation. Geothermics, 64, (2016), 235-245.

Hamm, V., Kervévan, C., and Thiéry, D.: CO2-DISSOLVED: A Novel Concept Coupling Geological Storage of Dissolved CO2 and Geothermal Heat Recovery–Part 4: Preliminary Thermo-Hydrodynamic Simulations to Assess the CO2 Storage Efficiency. Energy Procedia, 63, (2014), 4548-4560.

Huber, C., B. Shafei, and A. Parmigiani: A new pore-scale model for linear and non-linear heterogeneous dissolution and precipitation. Geochimica et Cosmochimica Acta, 124: (2014), p. 109-130.

Izgec, O., Demiral, B., Bertin, H., and Akin, S.: Calcite precipitation in low temperature geothermal systems: an experimental approach. In 30th Workshop on Geothermal Reservoir Engineering, Stanford University, Stanford, California, TR-176, (2005).

Jun, Y.S., Kim, D. and Neil, C.W.: Heterogeneous nucleation and growth of nanoparticles at environmental interfaces. Accounts of chemical research, 49(9), (2016), pp.1681-1690.

Kaczmarek, S. and Thornton, B.: The effect of temperature on stoichiometry, cation ordering, and reaction rate in high-temperature dolomitization experiments. Chemical Geology, 468, (2017), pp.32-41.

Kiryukhin, A., Xu, T., Pruess, K., Apps, J., and Slovtsov, I.: Thermal–hydrodynamic–chemical (THC) modeling based on geothermal field data. Geothermics, 33(3), (2004), 349-381.

Koehn, D., Lindenfeld, M., Rümpker, G., Aanyu, K., Haines, S., Passchier, C. W., and Sachau, T.: Active transsection faults in rift transfer zones: evidence for complex stress fields and implications for crustal fragmentation processes in the western branch of the East African Rift. International Journal of Earth Sciences, 99(7), (2010), 1633-1642.

Landrot, G., Ajo-Franklin, J.B., Yang, L., Cabrini, S. and Steefel, C.I.: Measurement of accessible reactive surface area in a sandstone, with application to CO2 mineralization. Chemical Geology, 318, (2012), pp.113-125.

Li, D., Nielsen, M. H., Lee, J. R., Frandsen, C., Banfield, J. F., and De Yoreo, J. J.: Direction-specific interactions control crystal growth by oriented attachment. Science, 336(6084), (2012), 1014-1018.

Li, Q., Fernandez-Martinez, A., Lee, B., Waychunas, G. A., and Jun, Y. S.: Interfacial energies for heterogeneous nucleation of calcium carbonate on mica and quartz. Environmental science & technology, 48(10), (2014), 5745-5753.

Liu, C., et al.: Pore-scale process coupling and effective surface reaction rates in heterogeneous subsurface materials. Rev Mineral Geochem. 80: (2015), p. 191-216.

McGraw, R. L., Winkler, P. M., and Wagner, P. E.: Temperature dependence in heterogeneous nucleation with application to the direct determination of cluster energy on nearly molecular scale. Scientific reports, 7(1), 16896, (2017).

McNamara, D. D., Lister, A., and Prior, D. J.: Calcite sealing in a fractured geothermal reservoir: Insights from combined EBSD and chemistry mapping. Journal of Volcanology and Geothermal Research, 323, (2016), 38-52.

Mella, M., Rose, P., Kovac, K., Xu, T., and Pruess, K.: Calcite dissolution in geothermal reservoirs using chelants. Geothermal Resources Council Transactions 30, (2006), 347–352

Michaelides, A., and Scheffler, M.: An introduction to the theory of crystalline elemental solids and their surfaces. Surface and Interface Science, 1, (2012).

Morley, C. K.: How successful are analogue models in addressing the influence of pre-existing fabrics on rift structure?. Journal of Structural Geology, 21(8-9), (1999), 1267-1274.

Mountassir, G.E., Lunn, R.J., Moir, H. and MacLachlan, E.: Hydrodynamic coupling in microbially mediated fracture mineralization: Formation of self-organized groundwater flow channels. Water Resources Research, 50(1), (2014), pp.1-16.

Okamoto, A., and Tsuchiya, N.: Velocity of vertical fluid ascent within vein-forming fractures. Geology, 37(6), (2009), 563-566.

Parsons, S., Wang, B., Judd, S. and Stephenson, T.: Magnetic treatment of calcium carbonate scale—effect of pH control. Water Research, 31(2), (1997), pp.339-342.

Portier, S., Vuataz, F., Nami, P., Sanjuan, B. and Gérard, A.: Chemical stimulation techniques for geothermal wells: experiments on the three-well EGS system at Soultz-sous-Forêts, France. Geothermics, 38(4), (2009), pp.349-359.

Prior, D. J., Mariani, E., and Wheeler, J.: EBSD in the earth sciences: applications, common practice, and challenges. In Electron backscatter diffraction in materials science (pp. 345-360). Springer, Boston, MA, (2009).

Ringe, E., Van Duyne, R. P., and Marks, L. D.: Kinetic and thermodynamic modified Wulff constructions for twinned nanoparticles. The Journal of Physical Chemistry C, 117(31), (2013), 15859-15870.

Rothbaum, H. P., Anderton, B. H., Harrison, R. F., Rohde, A. G., and Slatter, A.: Effect of silica polymerisation and pH on geothermal scaling. Geothermics, 8(1), (1979), 1-20.

Schobesberger, S., Winkler, P. M., Pinterich, T., Vrtala, A., Kulmala, M., and Wagner, P. E.: Experiments on the Temperature Dependence of Heterogeneous Nucleation on Nanometer-Sized NaCl and Ag Particles. ChemPhysChem, 11(18), (2010), 3874-3882.

Sonney, R. and Mountain, B.W.: Experimental simulation of greywacke–fluid interaction under geothermal conditions. Geothermics, 47, (2013), pp.27-39.

Taron, J. and Elsworth, D.: Thermal–hydrologic–mechanical–chemical processes in the evolution of engineered geothermal reservoirs. International Journal of Rock Mechanics and Mining Sciences, 46(5), (2009), pp.855-864.

Tartakovsky, A.M., et al.: A smoothed particle hydrodynamics model for reactive transport and mineral precipitation in porous and fractured porous media. Water Resour. Res. 43(5): p. W05437, (2007).

Urai, J.L., Williams, P.F. and Van Roermund, H.L.M.: Kinematics of crystal growth in syntectonic fibrous veins. Journal of Structural Geology, 13(7), (1991), pp.823-836.

Virransalo, P., P. Härmä, J. Pokki, T. Manninen, M. Lehtonen, and T. Koistinen: Geological map of Uganda, Hoima, Sheet N°NA-36-9: GTK Consortium, (2012).

Walters, B.: Extensional Reservoirs: Examples of the lake's intracontinental rift Albert (Uganda) and the proximal margin of Ifni (Morocco). PhD. University of Lorraine, (2016).

Zhang, X., Shen, Z., Liu, J., Kerisit, S. N., Bowden, M. E., Sushko, M. L., ... and Rosso, K. M.: Direction-specific interaction forces underlying zinc oxide crystal growth by oriented attachment. Nature communications, 8(1), (2017), 835.